

RADIO AND GAMMA-RAY PULSED EMISSION FROM MILLISECOND PULSARS

Y. J. DU^{1,2}, G. J. QIAO³ AND D. CHEN¹

Accepted for publication in The Astrophysical Journal

ABSTRACT

Pulsed γ -ray emission from millisecond pulsars (MSPs) has been detected by the sensitive *Fermi*, which sheds light on studies of the emission region and mechanism. In particular, the specific patterns of radio and γ -ray emission from PSR J0101-6422 challenge the popular pulsar models, e.g. outer gap and two-pole caustic (TPC) models. Using the three dimension (3D) annular gap model, we have jointly simulated radio and γ -ray light curves for three representative MSPs (PSR J0034-0534, PSR J0101-6422 and PSR J0437-4715) with distinct radio phase lags and present the best simulated results for these MSPs, particularly for PSR J0101-6422 with complex radio and γ -ray pulse profiles and for PSR J0437-4715 with a radio interpulse. It is found that both the γ -ray and radio emission originate from the annular gap region located in only one magnetic pole, and the radio emission region is not primarily lower than the γ -ray region in most cases. In addition, the annular gap model with a small magnetic inclination angle instead of “orthogonal rotator” can account for MSPs’ radio interpulse with a large phase separation from the main pulse. The annular gap model is a self-consistent model not only for young pulsars but also MSPs, and multi-wavelength light curves can be fundamentally explained by this model.

Subject headings: pulsars: general — gamma rays: stars — pulsars: individual (J0034-0534, J0101-6422, J0437-4715) — radiation mechanisms: non-thermal — acceleration of particles

1. INTRODUCTION

MSPs are a population of old neutron stars with short spin period $P_0 \lesssim 20$ ms and small characteristic magnetic field $B_0 < 10^9$ G (actually small period derivative $\dot{P} \lesssim 10^{-17}$ s s⁻¹). They are believed to be formed from the recycling (accretion spin-up) process in binaries (Bhattacharya & van den Heuvel 1991). Furthermore, there is another possible formation channel for MSPs (even for sub-millisecond pulsars), that is accretion-induced collapse of white dwarfs in a binary (Nomoto & Kondo 1991; Du et al. 2009). Because of the high stability of their rotations, MSPs have great potential for application: autonomous deep-space navigation, pulsar-based time scale, low-frequency gravitational wave detection and so on.

When the first MSP, PSR B1937+21, had been discovered in 1982 (Backer et al. 1982), Usov (1983) soon predicted that this pulsar could emit γ -rays via synchrotron radiation on the order of 100 GeV. Bhattacharya & Srinivasan (1991) subsequently calculated the γ -ray luminosity of MSPs, estimated their contribution to the diffuse γ -ray background of the Milky Way, and finally discussed detectability of MSPs as point γ -ray sources. Using the data of *Energetic Gamma Ray Experiment*, Kuiper et al. (2000) showed circumstantial evidence for the likely detection of pulsed γ -ray emission from a MSP, PSR J0218+4232, which was regarded as a γ -ray pulsar candidate for a long time. MSPs’ γ -ray emission was not observationally confirmed until *Fermi* with a sensitive Large Area Telescope (LAT) launched in June of 2008. Using eight-month data of *Fermi* LAT, eight γ -ray MSPs have already been detected (Abdo et al. 2009). This number has grown to more than 40 up to date (Guillemot et al. 2012a), and still

increases.

From observations, MSPs are analogous to young pulsars, which have multi-wavelength pulsed emission from radio to γ -ray band. Do MSPs and young pulsars share a simple model that contains similar emission region and acceleration mechanism to self-consistently explain their multi-wavelength emission? More and more multi-wavelength data with high precision give us opportunities to obtain remarkable insights of the magnetospheric physics. The multi-wavelength study is a key method to discriminate the various pulsar non-thermal emission models for both MSPs and young pulsars.

Initially aiming to explain the high-energy pulsed emission from young pulsars, four traditional magnetospheric gap models have been suggested to study pulsed high energy emission of pulsars: the polar cap model (Daugherty & Harding 1994), the outer gap model (Cheng et al. 1986; Romani & Yadigaroglu 1995; Zhang & Cheng 1997), TPC/slot gap model (Dyks & Rudak 2003; Harding et al. 2008), and the annular gap model (Qiao et al. 2004, 2007; Du et al. 2010). To distinguish these pulsar models, the most important issues are the inducements of acceleration electric field region and related emission mechanisms to emanate high-energy photons (Du et al. 2011, 2012). One of the key discrepancies of the mentioned emission models is one-pole or two-pole emission pattern which depends on two corresponding geometry parameters: magnetic inclination angle α and viewing angle ζ .

Bulik et al. (2000) adopted the polar-cap model to calculate the γ -ray emission from MSPs. They pointed out that curvature radiation of primary particles contributed to the MeV-to-GeV band, while the synchrotron radiation arising from pairs dominated only below 1 MeV. Harding et al. (2005) developed the pair-starved polar cap model and obtain similar spectral conclusion for high-energy emission from MSPs as above. In this model the accelerating field is not screened and the entire open volume is available for particle acceleration and emission of gamma rays. Zhang & Cheng (2003) used

¹ National Space Science Center, Chinese Academy of Sciences, NO.1 Nanertiao, Zhongguancun, Haidian district, Beijing 100190, China; duyj@nssc.ac.cn

² National Astronomical Observatories, Chinese Academy of Sciences, jia 20 Datun Road, Beijing 100012, China

³ School of Physics, Peking University, Beijing 100871, China

the outer gap model with multi-pole magnetic field to model the X-ray and γ -ray spectra for four MSPs, and the predicted results basically agree with the observations (Harding et al. 2005).

Along with radio observations supplying us with excellent timing solutions for *Fermi* MSPs, the derived γ -ray and radio light curves with high signal-to-noise allow us to do joint simulation which can justify the pulsar emission models. Recently, Venter et al. (2009) simulated both radio and γ -ray light curves for MSPs in the pair-starved polar cap, TPC and outer gap models, and they found that most of their simulated light curves are well explained by the TPC and outer gap models. They especially simulated light curves for a minor group of MSPs with phase-aligned radio and γ -ray pulse profiles (Venter et al. 2012). In addition, Johnson et al. (2012) also used the geometric slot gap, outer gap model or pair-starved polar cap model to fit γ -ray and radio light curves for three MSPs.

A MSP PSR J0101-6422 with complex radio and γ -ray light curves, challenge the popular TPC and outer gap models (Kerr et al. 2012). It is found that neither of the two models can faithfully reproduce the observed light curves and phase lags. For such a complex radio profile the simple beam model they used may have been insufficient.

In this paper, we use a 3D annular gap model to study both radio and γ -ray light curves for three MSPs which stand for the relevant types of MSPs with different radio lags. In § 2, the annular gap and core gap will be simply introduced and the acceleration electric field in the annular gap is calculated. In § 3, we jointly simulate radio and γ -ray band light curves for PSR J0034-0534, J0101-6422 and J0437-4715. The radio phase lags are identified and the reasons for them explored. The conclusions and discussions are shown in § 4.

2. THE ANNULAR GAP AND CORE GAP FOR MSPS

2.1. The Definition of Annular Gap and Core Gap

In a pulsar magnetosphere (Goldreich & Julian 1969; Ruderman & Sutherland 1975), the critical field lines⁴ divide a polar cap into two distinct parts: the annular gap region and the core gap region (See Figure 1 of Du et al. 2012). The annular gap is constrained between the critical and last open field lines, and the core gap is around the magnetic axis and within critical field lines (Du et al. 2010). The size of the polar cap decreases with increasing spin period, but can be quite large for MSPs and young pulsars. The annular gap width is correspondingly larger for short spin-period pulsars, and it varies with the magnetic azimuth ψ . For an anti-parallel rotator and $\psi = 0^\circ$, the radii of the annular polar region is $r_{\text{ann}} = r_{\text{pc}} - r_{\text{core}} = 0.26R(\Omega R/c)^{1/2}$ (Du et al. 2010), here R is a pulsar's radius, and Ω is its angular spin frequency.

Combining advantages of the outer gap and TPC models, Qiao et al. (2004, 2007) originally suggested the annular gap model, which has been further developed by Du et al. (2010, 2011, 2012). The site for generation of high energy photons is mainly located in the vicinity of the null charge surface⁵. Being consistent with the physically calculated spectra (Du et al. 2011), the Gaussian emissivities are numerically assumed when simulating light curves. The key emission geometry parameters α and ζ are not convincingly confirmed so

⁴ They are defined as a set of special field lines that satisfy the condition of $\Omega \cdot \mathbf{B} = 0$ at the light cylinder.

⁵ It is defined as a surface where the Goldreich-Julian (GJ) charge density ρ_{GJ} (Goldreich & Julian 1969) is zero.

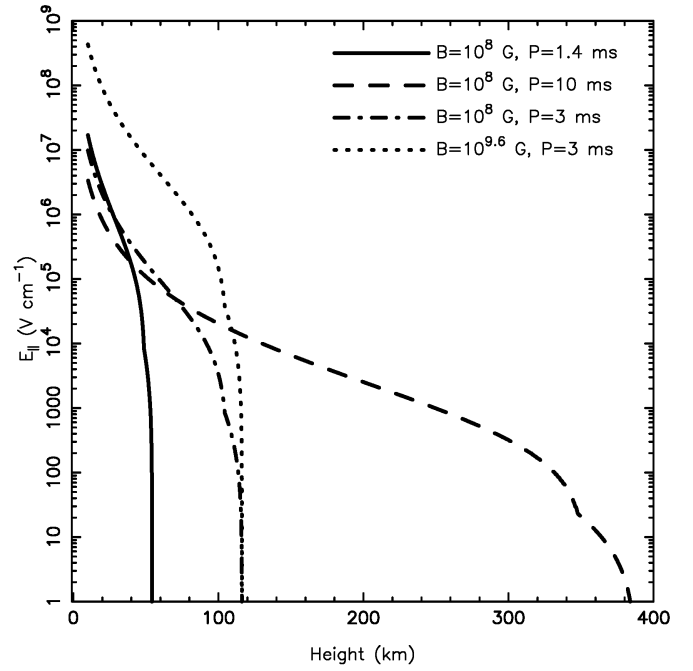


FIG. 1.— The calculated acceleration electric field on an open field line in the annular gap are plotted for typical MSPs with four groups of parameters of surface magnetic field B and spin period P . The electric field can extend from the pulsar surface to the null charge surface or even beyond it. The maximum electric field in the annular gap is sufficiently high to accelerate primary particles to ultra-relativistic energies.

far, we adopt these two values from related literature if they exist. If there are not any reliable values, we just use some random values according to theories of MSPs' magnetic field evolution. By hypothesizing reasonable emissivities and the magnetic inclination angle, this model can make wide fan-like emission beams, thus well reproduce the relevant light curves cut by a suitable viewing angle.

2.2. Acceleration Electric Field

Co-rotating charge-separated plasma is filled in a pulsar magnetosphere (Goldreich & Julian 1969; Ruderman & Sutherland 1975). When reaching some regions near the light cylinder, charged particles can not exceed the speed of light (c), thus escape from the magnetosphere. To compensate the escaping particles, the pulsar has to supply sufficient charged particles to its magnetosphere. This dynamic process continuously happens, thus a huge acceleration electric field is generated in the magnetosphere. This is the general mechanism for acceleration electric field (E_{\parallel}), which is suitable for both young pulsars (Du et al. 2011, 2012) and MSPs. The charged particles with opposite signs are simultaneously exporting from the annular gap and core gap, and satisfies the condition of circuit closure in the whole magnetosphere.

We assume the flowing-out particles' charge density equals to the local Goldreich-Julian density (Goldreich & Julian 1969) at a radial distance of $r \sim R_{\text{LC}}$, here $R_{\text{LC}} = \frac{cP}{2\pi}$ is a radius of light cylinder. The detailed calculation method and formulae are presented in Du et al. (2011). The acceleration electric fields of typical MSPs are shown in Figure 1 using four sets of surface magnetic field B and spin period P . For MSPs with large or small values of P and B , we found that, in all cases, the electric field in the inner region of the annular gap is sufficiently high ($E_{\parallel} \gtrsim 10^6 \text{ V cm}^{-1}$).

The charged particles accelerated in the annular gap or core gap are flowing out along a field line in a quasi-steady state. Using the derived acceleration electric field, we can obtain the Lorentz factor Γ_p of primary particles from the balance of acceleration and curvature radiation reaction

$$\Gamma_p = \left(\frac{3\rho^2 E_{\parallel}}{2e} \right)^{\frac{1}{2}} = 2.36 \times 10^7 \rho_7^{0.5} E_{\parallel,6}^{0.25},$$

where e is the charge of an electron, ρ_7 the curvature radius in units of 10^7 cm and $E_{\parallel,6}$ the acceleration electric field in units of 10^6 V cm $^{-1}$.

The primary particles are accelerated to ultra-relativistic energy with typical Lorentz factors of $\Gamma_p \sim 10^6 - 10^7$, because of the huge acceleration electric field in the annular gap. Since a lot of γ -ray photons are generated by the primary particles via curvature radiation and inverse Compton scattering processes, abundant e^{\pm} pairs are subsequently created through two-photon annihilation and photon-magnetic-absorption (γ -B) processes.

3. SIMULATING RADIO AND γ -RAY LIGHT CURVES FOR MSPS

Thanks to the *Fermi*-LAT, we now know that some MSPs are multi-wavelength emitters which have detectable radio and γ -ray pulsed emission. According to the observations of phase lag (Δ) between radio peak and γ -ray peak (Abdo et al. 2010a; Kerr et al. 2012), MSPs can be divided into four classes. PSR J0034-0534 represents a class of MSPs which has phase-aligned light curves ($\Delta \sim 0$); PSR J0101-6422 stands for another class which has moderate radio phase lag $\Delta \sim 0.2 - 0.3$ with quite complex radio or γ -ray light curves; PSR J0437-4715 stands for a third class which has larger radio lag $\Delta \sim 0.43$ and PSR J1744-1134 is a fourth class of MSPs whose γ -ray peak precedes the radio peak (Abdo et al. 2010a), we will model this MSP in future when high signal-to-noise γ -ray light curves are available. We process *Fermi* Pass 7 data to derive the observed light curves for three MSPs according to the radio timing solutions of MSPs from Fermi Science Support Center (FSSC)⁶. We select events with energies of > 0.1 GeV within 2° of each MSP's position and with zenith angles smaller than 105° . The key filter conditions for good time interval are rock angle $< 52^\circ$ and $\text{angsep}(\text{RA}_{\text{MSP}}, \text{DEC}_{\text{MSP}}, \text{RA}_{\text{SUN}}, \text{DEC}_{\text{SUN}}) < 5^\circ$, where RA and DEC are right ascension and declination respectively. Then we use tempo2 (Hobbs et al. 2006) with *Fermi* plug-in to obtain the spin phase for each photon. Finally we obtain the high signal-to-noise γ -ray light curves for the three MSPs (see red lines in Figure 2, 3, 4).

A convincing model should have simple clear emission geometric picture with reasonable input parameters, which can not only reproduce multi-wavelength light curves for young pulsars but also for MSPs. In this paper, we will jointly simulate radio and γ -ray light curves for PSR J0034-0534, PSR J0101-6422 and PSR J0437-4715. We briefly introduce the simulation method here. As shown in table 1, α and ζ are “first-rank” parameters, which are primarily adopted from the literature if they exist. When there are not any convincing values, we tend to use reasonable values of α from relevant theory on magnetic field evolution of pulsars (Ruderman 1991) and ζ is adopted randomly according to the simulated emission pattern (photon sky-map). When α and ζ are fixed,

several other model parameters are carefully adjusted for the emission regions until the observed light curve of the corresponding band can be reproduced. The model parameters for three MSPs are listed in table 1.

3.1. PSR J0034-0534

PSR J0034-0534 is the ninth γ -ray MSP detected by the *Fermi*-LAT (Abdo et al. 2010b), and it has strong γ -ray and radio pulsed emission with phase-aligned light curves. To reveal the emission region of this MSP, we use the annular gap model to jointly model the radio and γ -ray light curves. The simulation method is the same as described in §3.1 of Du et al. (2011). The key idea is to project all radiation intensities in both the annular gap and core gap to the “non-rotating” sky, considering some physical effects (e.g. aberration effect and retardation effect). Here we use numerical emissivities to speed up the calculations, since the assumed emissivities are consistent with the physically calculated spectra, as shown in Figure 8 of Du et al. (2011).

From Figure 2, we find that both radio and γ -ray emission are mainly generated in the annular gap region co-located at intermediate altitudes $r \sim 0.24 - 0.56R_{\text{LC}}$, which leads to the phase-aligned light curves. Abdo et al. (2010b) used the TPC and outer gap geometric models with $\alpha = 30^\circ$ and $\zeta = 70^\circ$ to obtain the light curves for PSR J0034-0534, and they derived similar conclusions that radio emission region extends from $0.6R_{\text{LC}}$ to $0.8R_{\text{LC}}$ and γ -ray region extends from $0.12R_{\text{LC}}$ to $0.9R_{\text{LC}}$. It is found that this MSP has a larger transverse emission region for radio emission. Moreover, Venter et al. (2012) developed the traditional outer gap and TPC model, adopting the similar idea of numerically assumed emissivity of piecewise-function, and derived the phase-aligned radio and γ -ray light curves for three MSPs including PSR J0034-0534. It seems that PSR J0034-0534 has off-peak pulsed γ -ray emission up to 100% duty cycle (Ackermann et al. 2011), which is not reproduced by the annular gap model. This might be due to the lack of knowledge on emission geometry and magnetic field configuration, and we will further develop our model to study this MSP in detail in the future.

3.2. PSR J0101-6422

The observed light curves of PSR J0101-6422 have complex features: the γ -ray profile is likely to have three peaks; while the radio profile contains three peaks that occupy nearly the whole rotation phase (see left panels of Figure 3). To well model both light curves, we consider both cases of single-pole and two-pole emission-picture with many attempts on a large number of parameter space. The light curves of this MSP favor a single-pole emission picture with $\alpha = 30^\circ$ and $\zeta = 48^\circ$, and the results are shown in Figure 3. For a viewing angle of $\zeta = 48^\circ$, the radio interpeak originates from the core gap with high altitudes of $0.3R_{\text{LC}}$ to $0.7R_{\text{LC}}$; while the other two peaks with a bridge (at the phases of ~ -0.3 and ~ 0.45) originate from the annular gap with altitudes of $0.45R_{\text{LC}}$ to $0.78R_{\text{LC}}$. The γ -ray profile is similar, the interpeak (at phase of ~ 0) mainly originates from the core gap with high altitudes of $0.32R_{\text{LC}}$ to $0.6R_{\text{LC}}$, while the other two peaks originate from the annular gap with altitudes of $0.08R_{\text{LC}}$ to $0.4R_{\text{LC}}$.

According to the annular gap model, we note that the radio emission from PSR J0101-6422 is quite asymmetric in magnetic azimuth. This is possibly due to the special physical coherence condition and propagation effects in the pulsar magnetosphere. We add some discussions on radio emission in §4.

⁶ <http://fermi.gsfc.nasa.gov/ssc/data/access/lat/ephems/>

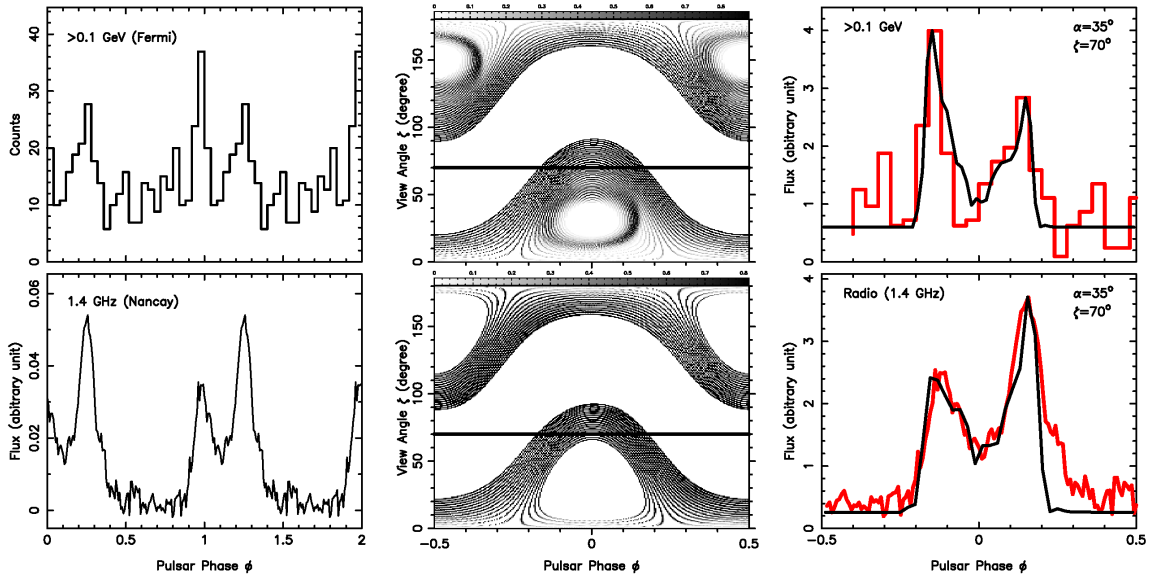


FIG. 2.— Simulated radio and γ -ray light curves for PSR J0034-0534. The observations are presented in the left panels, and the radio data is taken from the *Fermi* ephemeris website <http://fermi.gsfc.nasa.gov/ssc/data/access/lat/ephems/>. The photon sky-map (middle panels) for an inclination angle of $\alpha = 35^\circ$ and the corresponding simulated light curves (thin black lines in the right panels) for a viewing angle of $\zeta = 70^\circ$ are also presented, using the single-pole annular gap model that well reproduce the observed phase-aligned light curves (thick red lines in the right panels).

TABLE 1
MODEL PARAMETERS OF MULTI-WAVELENGTH LIGHT CURVES FOR THREE MSPS

Band	κ	λ	ϵ	σ_A	$\sigma_{\theta, A}$	σ_C	$\sigma_{\theta, C1}$	$\sigma_{\theta, C2}$
J0034-0534 ($\alpha = 35^\circ$; $\zeta = 70^\circ$)								
> 0.1 GeV	0.75	0.85	0.8	0.32	0.007	0.15	0.006	0.0052
Radio	—	—	0.58	—	0.013	—	0.00065	0.00053
J0101-6422 ($\alpha = 30^\circ$; $\zeta = 48^\circ$)								
> 0.1 GeV	0.50	0.85	0.8	0.3	0.009	0.15	0.006	0.006
Radio	—	—	1.5	—	0.006	—	0.0075	0.0078
J0437-4715 ($\alpha = 25^\circ$; $\zeta = 42^\circ$)								
> 0.1 GeV	0.1	0.1	1.3	0.03	0.002	0.02	0.001	0.001
Radio	—	—	1.2	—	0.0004	—	0.0002	0.0002

NOTE. — α and ζ are magnetic inclination angles and viewing angles; κ and λ are two geometry parameters to determine the peak altitude in the annular gap; ϵ is a parameter for the peak altitude in the core gap; σ_A and σ_C are length scales for the emission region on each open field line in the annular gap and the core gap in units of R_{LC} , respectively; $\sigma_{\theta, A}$ is the transverse bunch scale for field lines in the annular gap; $\sigma_{\theta, C1}$ and $\sigma_{\theta, C2}$ are the bunch scale for field lines of $-180^\circ < \psi_s < 90^\circ$ and $90^\circ < \psi_s < 180^\circ$ in the core gap, respectively. The detailed description of these symbols can be found in (Du et al. 2011).

3.3. PSR J0437-4715

PSR J0437-4715 is a very close MSP with a distance of 0.16 kpc to the Earth (Manchester et al. 2005), and has multi-wavelength emission. Chen et al. (1998) suggested that PSR J0437-4715 was an aligned rotator. We therefore adopted a relatively small magnetic inclination angle as $\alpha = 25^\circ$ and a reasonable viewing angle as $\zeta = 42^\circ$ from the high-precision radio timing observations (van Straten et al. 2001; Hotan et al. 2006). Bogdanov et al. (2007) also used the value of $\zeta = 42^\circ$ to successfully model the thermal X-ray pulsations of this MSP. We apply our annular gap model to jointly simulate its radio and γ -ray light curves, and the results are shown in Figure 4. We emphasize that the radio interpulse can be reproduced by our model, although it does not precisely match the observations. The radio emission including the main peak and interpulse originate from a much higher and narrower region in the annular gap region with high altitudes of $0.48R_{LC}$ to $0.57R_{LC}$; while the γ -ray emission is generated in the annular gap region with lower altitudes of $0.064R_{LC}$ to $0.15R_{LC}$ located in the same magnetic pole. This leads to a large radio lag of $\Delta \sim 0.43$.

4. CONCLUSIONS AND DISCUSSIONS

Pulsed γ -ray emission from MSPs has been observed by the sensitive *Fermi*-LAT. Particularly, the specific pattern of radio and γ -ray emission from the PSR J0101-6422 challenges the outer gap and TPC models. A convincing model should apply not only to young pulsars but also to MSPs. In this paper, we used the annular gap model to jointly model the radio and γ -ray light curves for three representative MSPs PSR J0034-0534, PSR J0101-6422 and PSR J0437-4715 with distinct radio phase lags. For PSR J0034-0534 with phase-aligned radio and γ -ray light curves, both bands are mainly generated in the annular gap region co-located at intermediate altitudes. For PSR J0101-6422 with complex radio and γ -ray pulse profiles, we presented the best simulated results for this type of MSPs. The radio interpulse originate from the core gap at higher altitudes; while the other two radio peaks with a bridge originate from the annular gap region. The interpeak originates from the core gap region and the other two peak from the annular gap region. For PSR J0437-4715 with a large radio lag, the radio emission (including the interpulse) originates from a much higher and narrower region in the annular gap region,

Annular Gap Model for MSPs

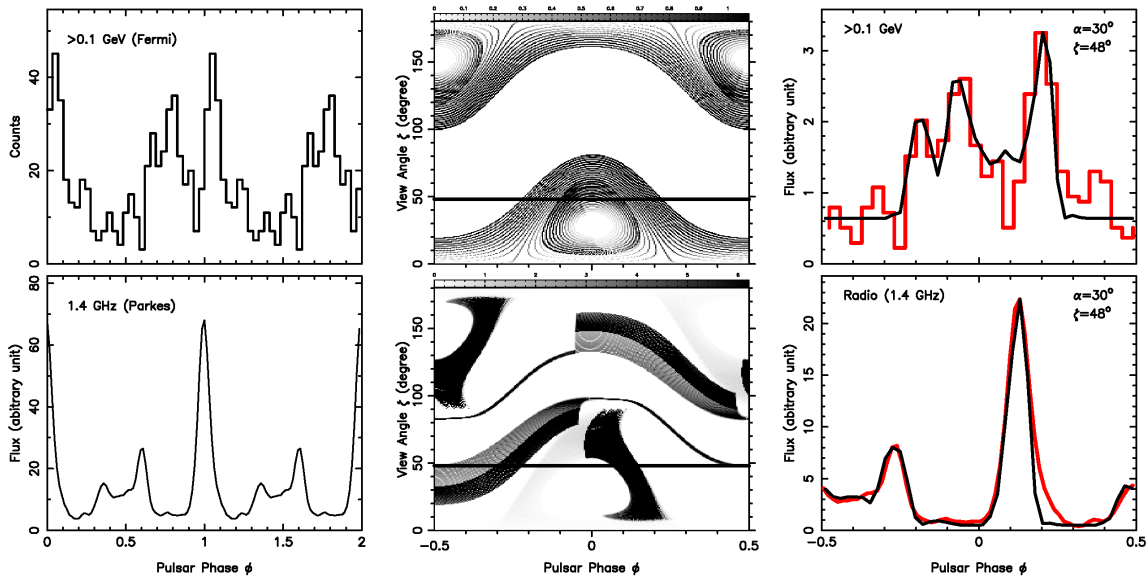


FIG. 3.— Similar as Figure 2, but for PSR J0101-6422. The radio data is obtained from Kerr et al. (2012). The inclination angle $\alpha = 30^\circ$ and viewing angle $\zeta = 48^\circ$ are used to model the complex radio and γ -ray light curves with moderate radio lag for this distinct MSP.

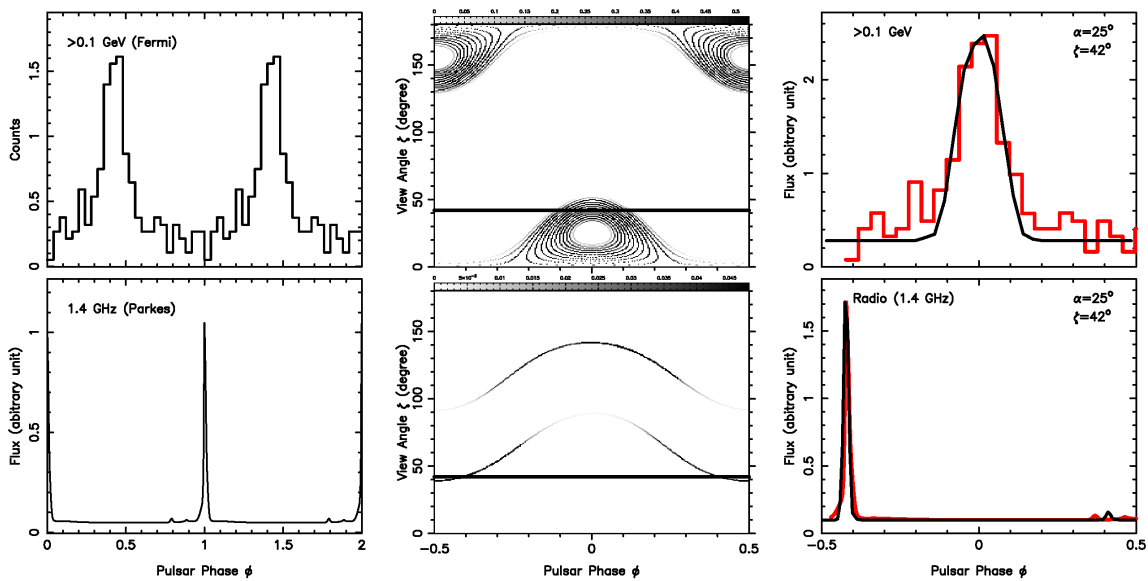


FIG. 4.— Similar as Figure 2, but for PSR J0437-4715. From right bottom panel, the radio interpulse at phase ~ -0.4 and main peak at phase ~ 0.4 are reproduced by the annular gap model, and they are generated from a higher and narrower region in the annular gap region of the same magnetic pole as the γ -ray emission. The radio profile for this MSP is observed from Kunming 40-meter radio telescope (Hao et al. 2010). The inclination angle $\alpha = 25^\circ$ and viewing angle $\zeta = 42^\circ$ are used.

and the γ -ray emission has lower altitudes.

From simulations of these MSPs, the annular gap model favors a single-pole emission pattern with small inclination angles ($\alpha \lesssim 35^\circ$) for MSPs. This result is compatible with theories of magnetic field evolution of MSPs in binaries: some recycled pulsars tend to have aligning magnetic field moment, i.e. small magnetic inclination angle α (Ruderman 1991; Chen et al. 1998). Lamb et al. (2009) presented a concrete discussion on the α evolution of MSPs while they were recycling in low mass X-ray binaries, and they note that the strong interactions between spinning superfluid neutrons and magnetized superconducting protons in a pulsar's core force the spin axis to change. A MSP would be an aligned rotator ($\alpha \sim 0^\circ$) if the star's north and south magnetic poles are forced toward opposite spin poles by the accretion disk, or would be an or-

thogonal rotator ($\alpha \sim 90^\circ$) if both of the star's magnetic poles are forced toward the same spin pole. Moreover, it is certainly unclear what happens when a MSP's recycling process finishes, Young et al. (2010) analyzed the new pulse width data of normal pulsars, and found that the spin and magnetic axes would align when they spin down due to dipole radiation and particle outflowing.

Several MSPs are simply assumed to be nearly orthogonal rotators because they have a radio interpulse separated by a large phase of $\gtrsim 180^\circ$ from its main pulse (Chen et al. 1998). Guillemot et al. (2012b) studied multi-wavelength light curves for two MSPs (PSR B1937+21 and PSR B1957+20), and found that fitting the radio polarization data of PSR B1937+21 favors an orthogonal rotator. As with most RVM fits the confidence area is large but the orthogo-

nal configuration is further supported by the altitude-limited TPC and outer gap models. However, this is not universally true, at least in the case of the annular gap model. The radio light curve of MSPs (e.g. PSR J0437-4715) with an interpulse can be well explained by the annular gap model with a small magnetic inclination angle.

By simulating light curves for MSPs in the annular gap model, we found that the radio emission mainly originates from the high-altitude narrow region in the annular gap region. The radio emission pattern (photon sky-map) is patch-like in our model. The radio emissivities on each field line (in the annular gap or core gap) vary slightly (nearly uniform), but the case for γ -ray light-curve simulation is quite different, they vary a lot. High energy (γ -ray and X-ray) emission is generated by non-coherent radiation from relativistic primary particles and pairs, while radio emission is suggested to be generated by coherent radiation due to two-stream instability of outward and inward pairs (Ruderman & Sutherland 1975). Here we focus on studying radio and γ -ray light curves for MSPs, the concrete emission mechanism including polarization, spectral properties and long-term stabilities of radio lags are however needed to further study, considering the coherent condition and propagation effects. Han et al. (1998) systematically studied the radio circular polarization for pulsar integrated pulse profiles, and found that sense reversals of circular polarization are observed across the conal emission in some cases, unrestricted to core components. The polarization property of high-altitude radio emission from both annu-

lar and core gaps is a valuable subject to be investigated in future. We will keep on improving our model to present better simulated light curves, especially for the phases of leading wing of peak 1, trailing wing of peak 2 and off-peak pulses.

In this paper, we simulated radio and gamma-ray light curves for 3 MSPs. When high signal-to-noise data at other wavelengths is available in the future, we will re-simulate light curves and fit the multi-wavelength phase-resolved spectra. In sum, the annular gap model is a self-consistent model not only for young pulsars (Du et al. 2011, 2012), but also for MSPs, and multi-wavelength light curves can be well explained by this model.

The authors are very grateful to the referee for the insightful and constructive comments. We would like to appreciate Matthew Kerr very much for giving us the ephemeris and radio profile of PSR J0101-6422. YJD is supported by China Postdoctoral Science Foundation (Grant No.: 2012M510047), and partially supported by our institute project of ‘‘Five Key Foster Directions’’ (Grant No.: Y22116EA2S). GJQ is supported by the National Basic Research Program of China (2012CB821800) and National Natural Science Foundation of China (10833003). DC is supported by National Natural Science Foundation of China (10803006, 11010250) and Advance Research Projects of Space Science (Grant No.: XDA04070000).

Facilities: Fermi

REFERENCES

- Abdo, A. A., Ackermann, M., Ajello, M., et al. 2009, *Science*, 325, 848
 Abdo, A. A., et al. 2010a, *ApJS*, 187, 460
 Abdo, A. A., Ackermann, M., Ajello, M., et al. 2010b, *ApJ*, 712, 957
 Ackermann, M., Ajello, M., Baldini, L., et al. 2011, *ApJ*, 726, 35
 Backer, D. C., Kulkarni, S. R., Heiles, C., Davis, M. M., & Goss, W. M. 1982, *Nature*, 300, 615
 Bhattacharya, D., & van den Heuvel, E. P. J. 1991, *Phys. Rep.*, 203, 1
 Bhattacharya, D., & Srinivasan, G. 1991, *Journal of Astrophysics and Astronomy*, 12, 17
 Bogdanov, S., Rybicki, G. B., & Grindlay, J. E. 2007, *ApJ*, 670, 668
 Bulik, T., Rudak, B., & Dyks, J. 2000, *MNRAS*, 317, 97
 Cheng, K. S., Ho, C., & Ruderman, M. 1986, *ApJ*, 300, 500
 Chen, K., Ruderman, M., & Zhu, T. 1998, *ApJ*, 493, 397
 Daugherty, J. K., & Harding, A. K. 1994, *ApJ*, 429, 325
 Du, Y. J., Xu, R. X., Qiao, G. J., & Han, J. L. 2009, *MNRAS*, 399, 1587
 Du, Y. J., Qiao, G. J., Han, J. L., Lee, K. J., Xu, R. X. 2010, *MNRAS*, 406, 2671
 Du, Y. J., Han, J. L., Qiao, G. J., & Chou, C. K. 2011, *ApJ*, 731, 2
 Du, Y. J., Qiao, G. J., & Wang, W. 2011, *ApJ*, 748, 84
 Dyks, J., & Rudak, B. 2003, *ApJ*, 598, 1201
 Goldreich, P., & Julian, W. H. 1969, *ApJ*, 157, 869
 Guillemot, L., for the Fermi LAT Collaboration 2012a, arXiv:1210.5341
 Guillemot, L., Johnson, T. J., Venter, C., et al. 2012b, *ApJ*, 744, 33
 Han, J. L., Manchester, R. N., Xu, R. X., & Qiao, G. J. 1998, *MNRAS*, 300, 373
 Hao, L.-F., Wang, M., & Yang, J. 2010, *Research in Astronomy and Astrophysics*, 10, 805
 Harding, A. K., Usov, V. V., & Muslimov, A. G. 2005, *ApJ*, 622, 531
 Harding, A. K., Stern, J. V., Dyks, J., & Frackowiak, M. 2008, *ApJ*, 680, 1378
 Hobbs, G. B., Edwards, R. T., & Manchester, R. N. 2006, *MNRAS*, 369, 655
 Hotan, A. W., Bailes, M., & Ord, S. M. 2006, *MNRAS*, 369, 1502
 Johnson, T. J., Harding, A. K., Venter, C., et al. 2012, arXiv:1210.1504
 Kerr, M., Camilo, F., Johnson, T. J., et al. 2012, *ApJ*, 748, L2
 Kuiper, L., Hermsen, W., Verbunt, F., et al. 2000, *A&A*, 359, 615
 Lamb, F. K., Boutloukos, S., Van Wassenhove, S., et al. 2009, *ApJ*, 706, 417
 Manchester, R. N., Hobbs, G. B., Teoh, A., & Hobbs, M. 2005, *AJ*, 129, 1993
 Nomoto, K., & Kondo, Y. 1991, *ApJ*, 367, L19
 Qiao, G. J., Lee, K. J., Wang, H. G., Xu, R. X., & Han, J. L. 2004, *ApJ*, 606, L49
 Qiao, G. J., Lee, K. J., Zhang, B., Wang, H. G., & Xu, R. X. 2007, *Chin. J. Astron. Astrophys.*, 7, 496
 Romani, R. W., & Yadigaroglu, I.-A. 1995, *ApJ*, 438, 314
 Ruderman, M. A., & Sutherland, P. G. 1975, *ApJ*, 196, 51
 Ruderman, M. 1991, *ApJ*, 366, 261
 Usov, V. V. 1983, *Nature*, 305, 409
 van Straten, W., Bailes, M., Britton, M., et al. 2001, *Nature*, 412, 158
 Venter, C., Harding, A. K., & Guillemot, L. 2009, *ApJ*, 707, 800
 Venter, C., Johnson, T. J., & Harding, A. K. 2012, *ApJ*, 744, 34
 Young, M. D. T., Chan, L. S., Burman, R. R., & Blair, D. G. 2010, *MNRAS*, 402, 1317
 Zhang, L., & Cheng, K. S. 1997, *ApJ*, 487, 370
 Zhang, L., & Cheng, K. S. 2003, *A&A*, 398, 639